On the accuracy of RF positioning in multi-Capsule endoscopy

Yunxing Ye, Umair Khan, Nayef Alsindi, Ruijun Fu and Kaveh Pahlavan
Center for Wireless Information
Network Studies
Worcester Polytechnic Institute
Worcester, MA, 01609, USA
(yunxingye,uikhan,ruijun,kaveh)@wpi.edu, nayefalsindi@gmail.com

***Abstract*—In this paper, we derive and analyze cooperative localization bounds for endoscopic wireless capsule as it passes through the human gastrointestin (GI) tract. We derive the Cramer-Rao lower bound (CRLB) variance limits on location estimators which use measured received signal strength(RSS). Using a three-dimension human body model from a full wave simulation software and log-normal models for RSS propagation from implant organs to body surface, we calculate bounds on location estimators in three digestive organs: stomach, small intestine and large intestine. We provide analysis of the factors affecting localization accuracy including various organ environments, external sensor array topology and number of pills in cooperation. The simulation results show that the number of receiver sensors on body surface has more influence on the accuracy of localization than the number of pills in cooperation inside the GI tract.**

I. Introduction

Recently, wireless capsule endoscopy (WCE) has attracted lots of attention due to its non-invasive nature. Furthermore, it allows the physician to visualize the entire gastrointestinal (GI) tract without scope trauma and air insufflations. Traditional techniques such as gastroscopy and colonscopy can only reach the first few or last several feet of the GI tract. Despite the advantages the WCE have, it is reported that a physician spends one or two hours to assess the photos taken during each WCE examination, since approximately fifty thousands photos are taken during the eight hours period of examination [1]. This slows down the process of examination and increases the cost of the procedure significantly. Meanwhile, after the examination by WCE, the physician may want to revisit the sites of interest for further diagnosis or treatment. Accurate location information of the capsule can help in both reducing the time needed for assessing the photos and assisting the physicians for follow-up interventions.

Various technologies for localization of the capsule have been explored in feasibility studies. The original idea is to use a spatially scanning system to locate the points with the strongest RSS. The system is non-commercial and cumbersome. Frisch et al[2] developed a RF triangulation system using an external sensor array that measures signal strength of capsule transmissions at multiple points and uses this information to estimate the distance. The average experimental error is reported to be 37.7mm [3]. Other techniques include ultrasound [4], time of arrival (TOA) based pattern recognition [5], magnetic tracking [6],[7] and computer vision [8],[9].

Among these technologies, RF signal based localization systems have the advantage of application-non-specific and relatively low cost for implementation. Therefore, it has been chosen for use with the Smartpill capsule [10] in USA and the M2A capsule [11] in Israel. Generally, the RF localization technique is based on TOA, angle of arrival (AOA) or received signal strength (RSS) measurements. A widely known benefit of TOA based techniques is their high accuracy compared to RSS and AOA based techniques. However, the strong absorption of human tissue causes large errors in TOA estimation and the limited bandwidth (402-405MHz) of the Medical Implant Communication Services (MICS) band prevent us from high resolution TOA estimation. The problem is made even worse by the GI movement, and the filling and emptying cycle, resulting in unpredictable ranging error [12]. Thus, the ranging information from TOA estimation is not promising with the current technology.

The RSS based techniques are less sensitive to bandwidth limitation and harsh propagation environment.There are basically two ways to use the the RSS information for localization, triangulation and pattern recognition. In this paper, we only address the issues related to RSS triangulation techniques. RSS Triangulation technique is based on the path loss model from implant tissues to body surface. The model is used to calculate the distance between each external sensor and the capsule, then at least 4 link distances are used to calculate the location of the capsule in 3D space.

Currently, most of the researchers have focused on developing the algorithms and mathematical models for solving the triangulation problem [3],[13]. In this paper, we take a different approach. Based on the statistical implant path loss model developed in [14], we focus on the accuracy possible for capsules in the GI tract using RSS based triangulation technique, Yi etc have developed the localization bound calculation for single pill situation in [15]. The CRB presented in this paper quantify the limits of localization accuracy with certain reference-points topology, implant path loss model and number of pills in cooperation. Our aim is to analyze the accuracy achievable at various organs and determine if the accuracies are enough for endoscopy applications. Similar works have been done for indoor geolocation applications [16] and robot

localization applications [17].

We begin in Section II by summerizing the performance evaluation methodology which includes the scenario description and the implant to body surface path loss model for GI tract environment. Next, using the coordinates value from scenario and the path loss model, we derive the CRB for cooperative capsule localization in section III. In section IV, we provide results of simulation which highlight the network and organ location parameters that affect the localization accuracy. Finally, we conclude the paper in section V.

II. Performance Evaluation Methodology

1) Performance evaluation scenario: The GI tract consists of the esophagus, stomach, small intestine, and large intestine, as shown in Fig.1. In order to create a simulation scenario

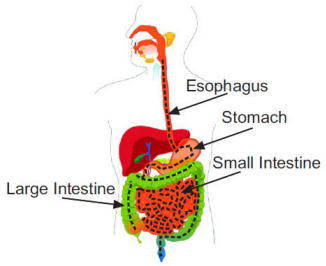

Fig. 1. A schematic of the GI tract. The typical path of a WCE is shown by the dashed black line

for calculating the CRB of wireless capsule as it travels through the human digestive system, we use a 3D human model from the three-dimensional full-wave electromagnetic field simulation system (Ansoft [18]). The 3D human body model has a spatial resolution of 2 millimeters and includes frequency dependent dielectric properties of 300+ parts in a male human body. We extract the 3D coordinates of digestive organs from the human body model, which is illustrated in fig. 2.

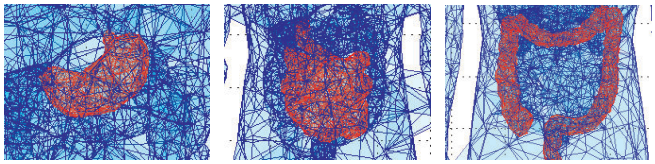

(a) Stomach (b) Small Intestine (c) Large Intestine

Fig. 2. Simulation scenarios

For the design of the topology of receiver sensors on body surface, we followed the idea in [2], assuming the receiver arrays are placed on a jacket wared by the patient during the examination. Same number of receivers are fixed in front and on the back of the jacket. We calculated the CRB for 8,16,32 and 64 receiver sensors with a three dimensional range of $268 \times 323 \times 312$millimeters, a typical network topology for 32 receiver sensors is illustrated in Fig.3

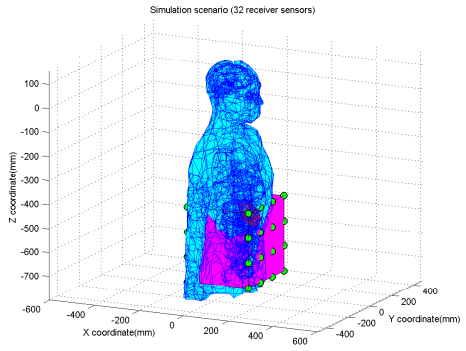

Fig. 3. WCE cooperative localization scenario

2) Path loss model for GI tract environment: In this subsection, we describe the statistical implant to body surface path loss model which is used for calculating the CRB of WCE localization. The model was developed by National Institute of Standards and Technology (NIST) at MICS band [14]. The main components used for developing the model include: a three-dimensional human body model, the propagation engine which is a three-dimensional full wave electromagnetic field simulator, the 3D immersive & visualization platform and implantable antenna.

The path loss in dB at some distance d between the transmitter and receiver can be statistically modeled by the following equation:

$$L_p(d) = L_p(d_0) + 10\alpha \log_{10}(d/d_0) + S(d > d_0) \quad (1)$$

where $d_0$is the reference distance (i.e. 50mm), and α is the path loss gradient which is determined by the propagation environment. For example, in free space, $\alpha = 2$. As we already mentioned, human body tissue strongly absorbs RF signal. Therefore, much higher value for the path loss gradient is expected. S is a random variable log-normally distributed around the mean which represents the deviation caused by shadowing effect of human tissue.

The parameters of the implant to body surface path loss model are summarized in table I.

TABLE I
Parameters for the statistical implant to body surface path loss model

Implant to Body Surface	$L_p(d_0)$(dB)	α	σ_{dB}
Deep Tissue	47.14	4.26	7.85
Near Surface	49.81	4.22	6.81

where σ_{dB} is the standard deviation of shadow fading S. Note that there are two sets of parameters for path loss from deep and near surface implant to body surface. During our simulation, we use 10cm distance between the transmitter and receiver on body surface as the threshold for choosing the model. If the distance is less than 10cm, we use the near surface to surface path loss model, otherwise the deep tissue to surface model is used, One illustration of how we select the models for various receiver sensors shown in Fig. 4

III. CRB for 3D capsule localization

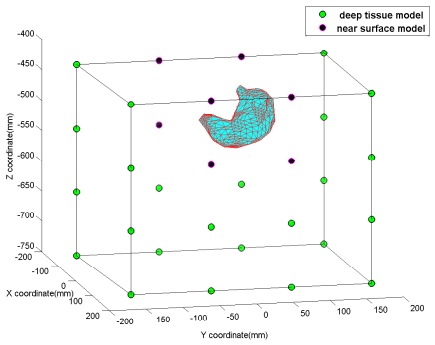

Fig. 4. Path loss model selection(32 receiver sensors, stomach)

Based on the path loss model in section II, we derive the 3D CRB for cooperative localization in WCE. The scenario we consider is as follows, N wireless endoscopic capsules are distributed in the digestive system with location given by $\theta_c = [p_1, ..., p_N]$. These pills are blindfolded devices but they can measure the RSS from each other and transmit the information out to the receiver array for further processing. M receiver sensors are placed on the surface of the human body with location given by $\theta_r = [p_{N+1}, ..., p_{N+M}]$. The vector of device parameters is $\theta = [\ \theta_c \quad \theta_r\ ]$. For this three dimensional system, $p_i = [x_i, y_i, z_i]^T$, where $i \in [1, N+M]$ and T is the transpose operation. The unknown parameters to be estimated can be represented by a $3 \times N$ coordinates matrix.

$$\theta_c = [p_1, p_2, ..., p_N] = \begin{bmatrix} x_1 & x_2 & ... & x_N \\ y_1 & y_2 & ... & y_N \\ z_1 & z_2 & ... & z_N \end{bmatrix} \tag{2}$$

Consider devices (devices include capsules and receivers)i and j make pair-wise observations $X_{i,j}$. We assume each receiver sensor can measure the RSS from all the capsules inside the body, but the path loss parameters for different links varies as the distance between the receiver sensor and capsule inside the body changes. Therefore, Let $H(i) = \{j$:device j makes pair-wise observations with device $i\}$. $H\{i\} = \{1, ...i-1, i+1, ...N+M\}$ for $i \in [1, N]$ and $H\{i\} = \{1, ...N\}$ for $i \in [N+1, N+M]$ because a device cannot make pairwise observation with itself and the receivers do not make observations with receivers either. Therefore the length of the observation vector X is $N \times (N+M-1) + M \times N$.

By reciprocity,we assume $X_{i,j} = X_{j,i}$; Thus, it is sufficient to consider only the lower triangle of the observation matrix X when formulating the joint likelihood function [19]. The CRB on the covariance matrix of any unbiased estimator $\hat{\theta}$ is given by [20]:

$$cov(\hat{\theta}) = E\left[(\hat{\theta} - \theta)(\hat{\theta} - \theta)^T\right] \geq F_\theta^{-1} \tag{3}$$

where $E[\cdot]$ is the expectation operation and F is the Fisher information matrix (FIM) defined as:

$$\begin{aligned} F_\theta &= -E\nabla_\theta(\nabla_\theta \ln f(X|\theta))^T \\ &= E_\theta[\tfrac{\partial}{\partial\theta} \ln f(X|\theta)(\tfrac{\partial}{\partial\theta} \ln f(X|\theta))^T] \\ &= \begin{bmatrix} F_{Rxx} & F_{Rxy} & F_{Rxz} \\ F_{Rxy}^T & F_{Ryy} & F_{Ryz} \\ F_{Rxz}^T & F_{Ryz}^T & F_{Rzz} \end{bmatrix} (3D \quad situation) \end{aligned} \tag{4}$$

where $f(X|\theta)$ is the joint PDF of the observation vector X conditioned on θ. For the RSS measurements case, the $X_{i,j}$ are log-normal random variables, and the density is given by [19]

$$\begin{aligned} f(X_{i,j}|p_i, p_j) &= \tfrac{10/\log 10}{\sqrt{2\pi\sigma_{dB}^2}} \tfrac{1}{X_{i,j}} \exp\left[-\tfrac{b}{8}(\log \tfrac{d_{i,j}^2}{\tilde{d}_{i,j}^2})^2\right] \\ b &= (\tfrac{10\alpha}{\sigma_{dB}})^2 \\ \tilde{d}_{i,j} &= d_0(\tfrac{X_0}{X_{i,j}})^{\frac{1}{\alpha}} \\ d_{i,j} &= \sqrt{(x_i - x_j)^2 + (y_i - y_j)^2 + (z_i - z_j)^2} \end{aligned} \tag{5}$$

for $i = 1, 2..., N+M$ and $j \in H(i)$, $\tilde{d}(i,j)$ is the MLE of range $d_{i,j}$ given received power $X_{i,j}$. Then the logarithm of the joint condition pdf is:

$$l(X|\theta) = \sum_{i=1}^{M+N} \sum_{j \in H_i j < i} \log f_{X|\theta}(X_{i,j}|p_i, p_j) \tag{6}$$

It is shown in [19] that the 2^{nd} partial derivative of (6) w.r.t θ_r and θ_s will be a summation of terms if θ_r and θ_s are coordinates of the same device k, but will be only one term if θ_r and θ_s are coordinates of different devices k and l, $k \neq l$. For example:

$$\begin{aligned} \tfrac{\partial^2 l(X|\theta)}{\partial x_k \partial z_k} &= -b\textstyle\sum_{i \in H(k)} \tfrac{(x_i - x_k)(z_i - z_k)}{d_{i,k}^4} \left[-\log \tfrac{d_{i,k}^2}{\tilde{d}_{i,k}^2} + 1\right] \\ \tfrac{\partial^2 l(X|\theta)}{\partial x_k \partial z_l} &= -bI_{H(k)}(l) \tfrac{(x_i - x_k)(z_i - z_k)}{d_{i,k}^4} \left[\log \tfrac{d_{i,k}^2}{\tilde{d}_{i,k}^2} - 1\right] \end{aligned} \tag{7}$$

where $I_{H(k)}(l) = 1$ if $l \in H(k)$ and 0 otherwise. Since $E(\frac{d_{i,k}^2}{\tilde{d}_{i,k}^2}) = 0$. Thus, the elements of F_θ are:

$$[F_{R_{xx}}]_{k,l} = \begin{cases} b\sum_{i \in H(k)} \frac{(x_k - x_i)^2}{d_{ki}^4} & k = l \\ -bI_{H(k)}(l)\frac{(x_k - x_l)^2}{d_{kl}^4} & k \neq l \end{cases} \tag{8}$$

$$[F_{R_{xy}}]_{k,l} = \begin{cases} b\sum_{i \in H(k)} \frac{(x_k - x_i)(y_k - y_i)}{d_{ki}^4} & k = l \\ -bI_{H(k)}(l)\frac{(x_k - x_l)(y_k - y_l)}{d_{kl}^4} & k \neq l \end{cases}$$

$$[F_{R_{xz}}]_{k,l} = \begin{cases} b\sum_{i \in H(k)} \frac{(x_k - x_i)(z_k - z_i)}{d_{ki}^4} & k = l \\ -bI_{H(k)}(l)\frac{(x_k - x_l)(z_k - z_l)}{d_{kl}^4} & k \neq l \end{cases}$$

$$[F_{R_{yy}}]_{k,l} = \begin{cases} b\sum_{i \in H(k)} \frac{(y_k - y_i)^2}{d_{ki}^4} & k = l \\ -bI_{H(k)}(l)\frac{(y_k - y_l)^2}{d_{kl}^4} & k \neq l \end{cases}$$

$$[F_{R_{yz}}]_{k,l} = \begin{cases} b\sum_{i\in H(k)} \frac{(y_k-y_i)(z_k-z_i)}{d_{ki}^4} & k=l \\ -bI_{H(k)}(l)\frac{(y_k-y_l)(z_k-z_l)}{d_{kl}^4} & k\neq l \end{cases}$$

$$[F_{R_{zz}}]_{k,l} = \begin{cases} b\sum_{i\in H(k)} \frac{(z_k-z_i)^2}{d_{ki}^4} & k=l \\ -bI_{H(k)}(l)\frac{(z_k-z_l)^2}{d_{kl}^4} & k\neq l \end{cases}$$

Let $\hat{x}_i, \hat{y}_i, \hat{z}_i$ be the unbiased estimation of x_i, y_i, z_i, the trace of the covariance of the ith location estimate is given by:

$$\begin{aligned} &\sigma_i^2 = tr\left\{cov_\theta(\hat{x}_i, \hat{y}_i, \hat{z}_i)\right\} \\ &= Var_\theta(\hat{x}_i) + Var_\theta(\hat{y}_i) + Var_\theta(\hat{z}_i) \\ &\geq \left[F_{R_{xx}} - (F_{R_{xy}}F_{R_{xz}}) \begin{pmatrix} F_{R_{yy}} & F_{R_{yz}} \\ F_{R_{yz}} & F_{R_{zz}} \end{pmatrix}^{-1} \begin{pmatrix} F_{R_{xy}} \\ F_{R_{xz}} \end{pmatrix}\right]^{-1}_{i,i} \\ &+ \left[F_{R_{yy}} - (F_{R_{xy}}F_{R_{yz}}) \begin{pmatrix} F_{R_{xx}} & F_{R_{xz}} \\ F_{R_{xz}} & F_{R_{zz}} \end{pmatrix}^{-1} \begin{pmatrix} F_{R_{xy}} \\ F_{R_{yz}} \end{pmatrix}\right]^{-1}_{i,i} \\ &+ \left[F_{R_{zz}} - (F_{R_{xz}}F_{R_{yz}}) \begin{pmatrix} F_{R_{xx}} & F_{R_{xy}} \\ F_{R_{xy}} & F_{R_{yy}} \end{pmatrix}^{-1} \begin{pmatrix} F_{R_{xz}} \\ F_{R_{yz}} \end{pmatrix}\right]^{-1}_{i,i} \end{aligned} \quad (9)$$

IV. Simulation Results

A. Setup

The simulation setup is based on the application of WCE requiring localization of capsule in stomach, small intestine and large intestine environments. Esophagus is not included as a simulation scenario because traditional upper endoscopy techniques are powerful enough to diagnose diseases in it. M receiver sensors are distributed evenly on the surface of the body torso, see figure 3. N capsule pills are then distributed inside the GI tract environment. Connectivity is assumed between capsule pills and the receiver sensors and among capsule pills. The path loss parameters are determined by the length of each connection as mentioned in section II.

For the analysis of the simulations, we compute the average RMS of the location error of each situation. For the case of N different capsule locations, the RMSE is computed by:

$$RMSE = \frac{\sqrt{\sum_{i=1}^{N} \sigma_{x_i}^2 + \sigma_{y_i}^2 + \sigma_{z_i}^2}}{N} \quad (10)$$

where $\sigma_{x_i}^2, \sigma_{y_i}^2$ and $\sigma_{z_i}^2$ are the variance of each coordinate value of the ith pill location.

B. Effect of organ shape and location

In this subsection, we evaluate the impact of the organ shape and location on localization accuracy. For the simulation, we fixed the number of receiver sensors to 32 and assumed only one single capsule in each organ. We calculated the 3D-CRB for all the possible location points inside each organ (634 points for stomach, 1926 points for small intestine and 3334 points for large intestine). Figure 5 shows the CDF comparison of location error bound in different organs.

Notice that the localization error for capsule in small intestine is apparently smaller than that in large intestine. The

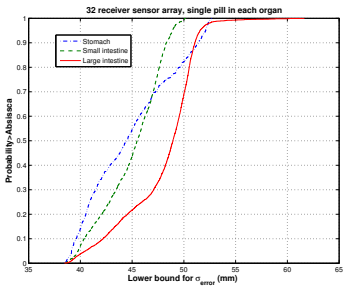

Fig. 5. CDF comparison of location error bound in stomach, small intestine and large intestine

average value of σ_{error} for small intestine environment is 45.5mm, while it is 49mm for large intestine environment. The localization error for capsule in stomach has the lowest average value but distributed in a wider range compared to the errors in other two environments. These observations can be explained by the geometric relationship between the sensor array and the organs. As we can see from fig. 4, stomach is located in the upper part of the receiver sensor array system, and its volume is the smallest among the three organs. Therefore, the localization error varies more in the stomach environment. The points located in the upper part of stomach have larger localization error value as they are far from the center of the receiver array system, the points in the lower part of stomach have smaller localization error value. The small intestine is located in the center part of human abdomen cavity and the lumen is more centralized compared to large intestine. Therefore, the localization error inside small intestine is smaller than that in large intestine.

C. Effect of number of receiver sensors

In this subsection, we investigate the impact of number of receiver sensors on localization accuracy. In this experiment, 12000 Monte Carlo simulations (3 different organs, 4 different number of receiver sensors and 1000 simulations per organ) were carried out with the number of receiver sensors varied from 8 64. During each simulation, we assume one capsule is located randomly inside each organ. The results show that the

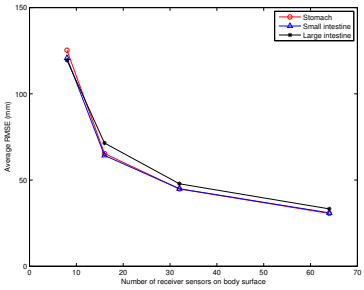

Fig. 6. Localization performances as a function of number of receiver sensors in different organs

number of receivers has significant influence on the accuracy of localization when the number of receivers is smaller than 32. The localization accuracy in small intestine is less sensitive to the number of receivers. This means that large intestine and

stomach are harsher implant environments for RF localization which requires more receiver sensors on body surface to achieve similar localization performance as environments with better geometric and channel condition. Finally, notice that for all the three organs, at least 32 receiver sensors are needed to guarantee the performance of 50mm average RMSE.

D. Effect of number of Pills in cooperation

Lastly, we investigate the impact of cooperation among pills. For this simulation, we fixed the number of receivers on body surface to 32 and increased the number of pills from 1 to 5. The pills are assumed to be randomly distributed inside each organ and they can measure the RSS from each other. 15000 simulations were carried out to study the effect of cooperation among pills. The results are presented in fig. 7. It is shown that

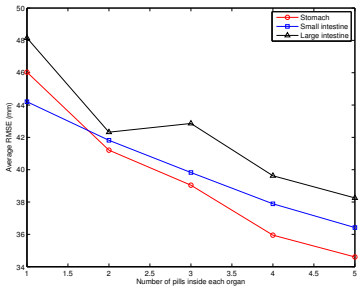

Fig. 7. Localization performances as a function of number of number of pills in different organs

as the number of pills increase from 1 to 5. the localization accuracy in all 3 organs improved, especially for large intestine and stomach environments. Localization accuracy in small intestine is again less sensitive to the number of pills which means it is a lighter environment for RF propagation and geometrically better surrounded by the receiver array. Notice that in practical situations, we do not want to send a lot of capsules into a patient due to the potential danger of digestion disorder and uncomfort for patient. Compared to the impact of number of receiver sensors, the number of pills in cooperation has less influence on the accuracy of localization. Therefore, our results indicate that increasing the number of receiver sensors on body surface is a more effective way to improve the overall localization performance than increasing the number of pills in cooperation for RSS based capsule localization.

V. Conclusion

In this paper, we investigated the potential accuracy limit for RSS triangulation based capsule localization in the human GI tract. We verified the possibility of achieving average localization error 50mm in the digestive organs. We also verified that more than 32 sensors on body surface is needed for achieving satisfying localization accuracy for capsule endoscopy. Simulation results showed that increasing the number of receiver sensors on body surface has more influence of the overall localization performance than increasing the number of pills inside the GI tract.Also considering the practical issues, we draw the conclusion that increasing the number of receiver sensors is a better way for reaching higher accuracy for capsule localization.

References

[1] J. Oh, S. K. Shah, X. Yuan, and S. J. Tang, "Automatic Classification of Digestive Organs in Wireless Capsule Endoscopy Videos," in *The 22nd Annual ACM Symposium on Applied Computing, SAC07*, Soul, 2007.

[2] M. Frisch, A. Glukhovsky, and D. Levy, "Array System and Method for Locating an in Vivo Signal Source," Patent US2002/0 173 718, May 20, 2002.

[3] M. Fischer, R. Schreiber, D. Levi, and R. Eliakim, "Capsule Endoscopy: the Localization System," *Gastrointestinal endoscopy clinics of north america*, vol. 14, pp. 25–31, 2004.

[4] K. Arshak and F. Adepoju, "Capsule Tracking in the GI Tract: A Novel Microcontroller Based Solution," in *IEEE sensors applications symposium*, 2006, pp. 186–191.

[5] M. Kawasaki and R. Kohno, "A TOA Based Positioning Technique of Medical Implanted Devices," in *Third international Symposium on Medical information & communication technology, ISMCIT09*, Montreal, 2009.

[6] X. Wang, M. Meng, and C. Hu, "A Localization Method Using 3-axis Magnetoresistive Sensors for Tracking of Capsule Endoscope," in *Proc. of IEEE/EMBS*, Soul, 2006, pp. 2522–2525.

[7] C. Hu, M. Meng, and M. Mandal, "The Calibratio of 3-axis Magnetic Sensor Array System for Tracking Wireless Capsule Endoscope," in *IEEE/RSJ International conference on robots and systems*, 2006, pp. 162–167.

[8] J. Bulat, K. Duda, M. Duplaga, R. Fraczek, A. Skalski, M. Socha, P. Turcza, and T. Zielinski, "Data Processing Tasks in Wireless GI Endoscopy: Image-based Capsule Localization and Navigation with Video Compression," in *Proc. of IEEE/EMBS*, 2007, pp. 2815–2818.

[9] R. Kuth, J. Reinschke, and R. Rockelein, "Method for Determing the Position and Orientation of an Endoscopy Capsule Guided Through an Examination Object by Using a Navigating Magnetic Field Generated by Means of a Navigation Device," Patent US2007/0 038 063, February 15, 2007.

[10] S. Thomas, "Smartpill Redefines 'Noninvasive'," in *Buffalo physician*, vol. 40, 2006, pp. 13–14.

[11] J. H, D. Levy, R. Shreiber, A. Glukhovsky, and D. Fisher, "Localization of the Given M2A Ingestible Capsule in the Given Diagnostic Imaging System," in *Gastrointestinal Endoscopy*, vol. 55, 2002, p. AB135.

[12] L. Wang, C. Hu, L. Tian, M. Li, and M. Q. H, "A Novel Radio Propagation Radiation Model for Localization of the Capsule in GI Tract," in *IEEE international conference on robotics and biomimetics*, December 19-23, 2009.

[13] K. Arshak and F. Adepoju, "Adaptive linearized methods for tracking a moving telemetry capsule," in *IEEE international symposium on industrial electronics (ISIE)*, June 2007, pp. 4–7.

[14] K. Sayrafian-Pour, W.-B. Yang, J. Hagedorn, J. Terrill, and K. Yazdandoost, "A statistical path loss model for medical implant communication channels," in *Personal, Indoor and Mobile Radio Communications, 2009 IEEE 20th International Symposium on*, 13-16 2009, pp. 2995 –2999.

[15] Y. Wang, R. Fu, Y. Ye, K. Umair, and K. Pahlavan, "Performance Bounds for RF Positioning of Endoscopy Camera Capsules," in *IEEE Radio and Wireless week*, Phoenix, Arizona, 2011.

[16] N. Alsindi and K. Pahlavan, "Cooperative localization bounds for indoor ultra-wideband wireless sensor networks," *EURASIP J. Adv. Signal Process*, vol. 2008, pp. 125:1–125:13, January 2008. [Online]. Available: http://dx.doi.org/10.1155/2008/852509

[17] N. Bargshady, K. Pahlavan, Y. Ye, F. Akgul, and N. Alsindi, "Bounds on Performance of Hybrid WiFi-UWB Cooperative Localization for Robotic Applications," in *Proceedings of IEEE International Symposium on Personal, Indoor and Mobile Radio Communications (PIMRC10)*, 2010.

[18] "Ansoft Full-wave electromagnetic Field Simulation," http://www.ansoft.com/products/hf/hfss/, [Online; accessed 27-September-2010].

[19] N. Patwari, I. Hero, A.O., M. Perkins, N. Correal, and R. O'Dea, "Relative location estimation in wireless sensor networks," *Signal Processing, IEEE Transactions on*, vol. 51, no. 8, pp. 2137 – 2148, aug. 2003.

[20] H. L. V. Trees, *Detection, Estimation, and Modulation Theory: Part I*. New York: Wiley, 1968.